*remote sensing*

MDPI

*Technical Note*

# Adjustment of Transceiver Lever Arm Offset and Sound Speed Bias for GNSS-Acoustic Positioning

**Guanxu Chen [1,2], Yang Liu [2], Yanxiong Liu [1,2,*], Ziwen Tian [2] and Menghao Li [2]**

[1] School of Geodesy and Geomatics, Wuhan University, Wuhan 430079, China
[2] First Institute of Oceanography, Ministry of Natural Resources, Qingdao 266061, China
* Correspondence: yxliu@fio.org.cn; Tel.: +86-532-88967067

Received: 14 May 2019; Accepted: 24 June 2019; Published: 5 July 2019


**Abstract:** Global Navigation Satellite System—Acoustic (GNSS-A) positioning is the main technique for seafloor geodetic positioning. A transceiver lever arm offset and sound velocity bias in seawater are the main systematic errors of the GNSS-A positioning technique. Based on data from a sea trial in shallow water, this paper studies the functional model of GNSS-A positioning. The impact of the two systematic errors on seafloor positioning is analysed and corresponding processing methods are proposed. The results show that the offset in the lever arm measurement should be parameterised in the observation equation. Given the high correlation between the vertical lever arm offset and the vertical coordinate of the seafloor station, a sample search method was introduced to fix the vertical offset correction. If the calibration of the sound velocity profiler cannot be ensured, the correction parameter of the sound velocity bias should be solved. According to the refined functional model and corrections, the position of a seafloor station in shallow water can be determined with a precision of better than 1 cm.

**Keywords:** GNSS-A; lever arm offset; sound velocity bias; sample search

## 1. Introduction

The Global Navigation Satellite System—Acoustic (GNSS-A) positioning technique combines the GNSS sea surface dynamic positioning technique and the underwater acoustic positioning technique [1,2], which is the important basis of marine science research and engineering surveys. As the main method of marine geodesy, the GNSS-A positioning technique can measure the displacement at plate boundaries [3]. Several great plate faults lie at the bottom of the ocean [4]. The information provided by the seafloor's precise positioning technique can not only be used to monitor the natural processes of the ocean, such as seafloor earthquakes, undersea volcanic eruptions, and tsunamis, but also enrich the modelling data of earth system science. The GNSS-A positioning technique also provides important technical support for marine oil and gas exploration and engineering construction [5]. The long baseline positioning system is the underwater acoustic navigation and positioning system with the widest coverage and the highest accuracy, whereas its application also requires the adoption of the GNSS-A positioning technique for the precise position calibration of its seafloor array [6–9].

At present, the accuracy of the seafloor position obtained by the GNSS-A positioning technique is limited by systematic errors, which mainly include the offset error of lever arms between shipborne devices and the bias of sound velocity measured in seawater [10,11]. The lever arm is the geometric vector in the ship-fixed coordinate system [12,13], which is used to transmit the GNSS dynamic positioning results to the acoustic transceiver centre. Because the actual installation position of the GNSS and acoustic devices is not completely the same as the planned position and direction in the ship's fixed coordinate system, there is an offset error in the lever arm installation [14]. Due to the influence of dynamic ocean processes, such as tides and internal waves, the sound velocity underwater

has temporal and spatial changes, which is especially irregular in the shallow sea [15–18]. Different from the electromagnetic waves of GNSS, which directly use the velocity of light as the velocity approximation, the velocity of the sound signal in seawater needs to be measured by professional equipment (the sound velocity profiler or CTD) [19]. Therefore, the systematic bias of the sound velocity is composed of an expression error, and a measurement error is introduced.

For transceiver lever arms, professional ships for marine geodesy install acoustic transceivers in the instrument well at the bottom of the middle of the ship [20], and the total station is used to measure the lever arm between the transceiver and GNSS positioning reference point with millimetre accuracy. Meanwhile, some teams attach transceivers and GNSS equipment to two ends of a pole that attach to one side of the ship [21,22], and it is assumed that there is only a vertical lever arm offset between the two sets of equipment, and the offset is considered to be measured precisely with no error. Generally, the transceiver and GNSS antenna are fixed at different positions of the ship [23–25]. In this situation, the transceiver is attached at the bottom of the pole on one side of the ship, while the GNSS is installed at the top of the ship. The lever arm between the two devices cannot be directly measured precisely, so the offset in the calculated range value is large.

For a sound velocity error, researchers in marine geodesy arrange the acoustic transponder array on a seafloor circle with the radius of water depth and can estimate the position changes of the array centre (virtual reference station) with centimetre-level accuracy by using shipborne GNSS and acoustic equipment [26,27]. Although the research of the virtual station is useful for the determination of the plate motion, which meets the needs of the geodetic survey, it is not specific to the precise position of each entity transponders; thus, its results are hard to be directly used in engineering construction and marine environment monitoring. Some scholars studied the positioning technology of the seafloor entity station composed of a single acoustic transponder, and proposed methods of optimising sailing tracks, processing methods of measurement differencing, and using distances between seafloor stations to build an adjustment model [28–30], which reduces the temporal and spatial correlation error and improves the positioning precision. However, few studies specifically discuss the systematic biases of the velocity of sound, including sound velocity measurement errors and temporal and spatial changes.

This paper deeply analysed the function model of the GNSS-A positioning technique for the single entity station and focused on the method of correcting systematic errors. Aiming at the problem of the high correlation between vertical coordinate/offset parameters and the bias of sound velocity measurements in the GNSS-A positioning, a sample search method was proposed to fix the lever arm offset in the vertical direction and detect the measurement error of sound velocity. By improving the GNSS-A positioning model, the sound velocity error and lever arm offset in equipment installation can be determined. Using shallow sea trial data, the GNSS-A positioning model was verified, and the transceiver lever arm offset and sound velocity bias were effectively corrected. Finally, the positioning accuracy of the seafloor station reached the centimetre level.

## 2. GNSS-A Positioning Model

GNSS-A positioning is a technique based on a range intersection, and the process is as follows. The position of the GNSS antenna can be obtained by utilizing GNSS technologies, and after transformation to the shipborne transceiver acoustic centre, the three-dimensional (3-D) coordinates of the seafloor station (transponder) can be calculated through the Euclidean distances converted from the travel time between the surface and seafloor acoustic equipment. Figure 1 shows the fundamental elements of this technique, in which the distance ($\rho$) between the shipborne acoustic transceiver and the seafloor transponder can be derived by the following:

$$\rho = \mathrm{vos} \cdot \frac{t}{2} = \sqrt{(x_{\mathrm{floor}} - x_{\mathrm{surface}})^2 + (y_{\mathrm{floor}} - y_{\mathrm{surface}})^2 + (z_{\mathrm{floor}} - z_{\mathrm{surface}})^2}, \quad (1)$$

where $t$ denotes the round-trip travel time, vos means the sound velocity of the sea area during the trial period. $x_{\mathrm{floor}}$, $y_{\mathrm{floor}}$ and $z_{\mathrm{floor}}$ epresent the coordinate components of the seafloor transponder

in the northing, easting, and height of the geodetic coordinate system, respectively, and they are the unknown parameters to be solved. $x_{\text{surface}}$, $y_{\text{surface}}$ and $z_{\text{surface}}$ enote the transceiver positions in the northing, easting, and height of the same coordinate system, respectively.

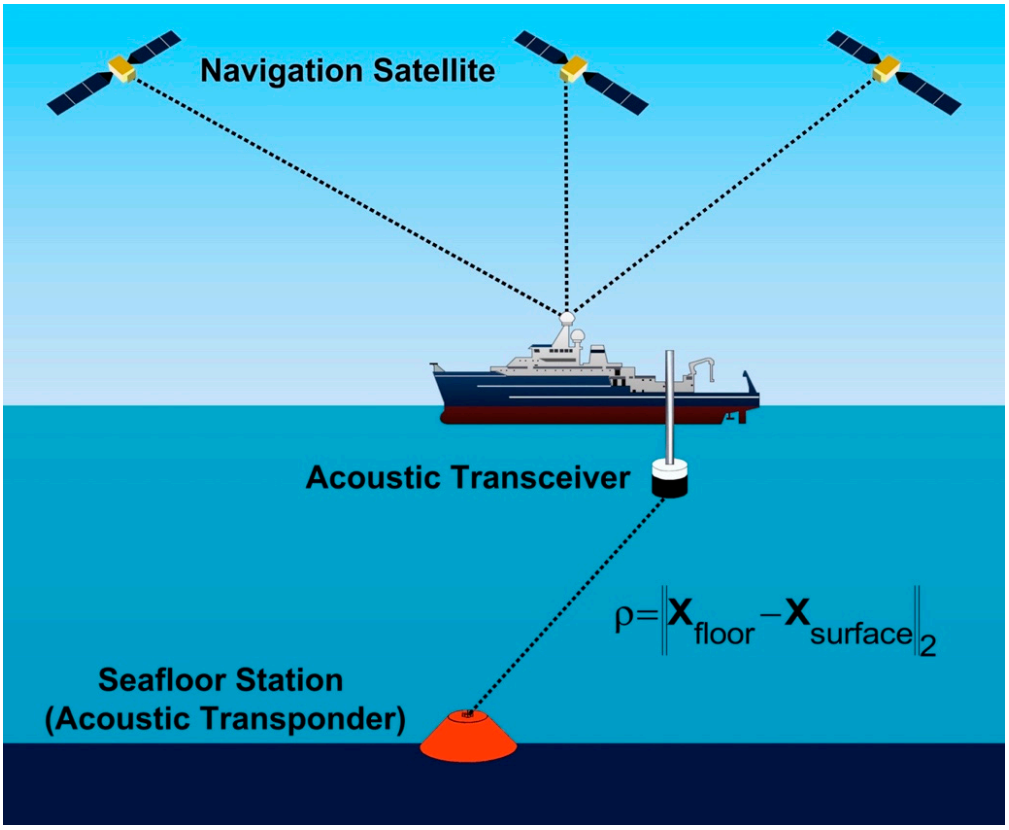


**Figure 1.** Principle of seafloor GNSS-Acoustic positioning.

As the acoustic transceiver and GNSS equipment are fixed on different positions of the ship, the position information should be transformed from the GNSS reference point to the acoustic transceiver centre. For the transformation, in addition to the GNSS positioning results, the ship attitude (heading, pitch, and roll) and lever arm between the transceiver and the GNSS reference point are also required. The position of the transceiver can be obtained based on the GNSS dynamic position results, lever arms, and rotation matrix:

$$\begin{bmatrix} x_{\text{surface}} \\ y_{\text{surface}} \\ z_{\text{surface}} \end{bmatrix} = \begin{bmatrix} x_{\text{GNSS}} \\ y_{\text{GNSS}} \\ z_{\text{GNSS}} \end{bmatrix} + \boldsymbol{R} \cdot \begin{bmatrix} \Delta x \\ \Delta y \\ \Delta z \end{bmatrix}, \tag{2}$$

where $x_{\text{GNSS}}$, $y_{\text{GNSS}}$, and $z_{\text{GNSS}}$ indicate the GNSS position results. $\Delta x$, $\Delta y$, and $\Delta z$ mean the lever arms from the GNSS equipment to the shipborne acoustic transceiver in the ship-fixed reference frame (with the origin at the GNSS reference point and a forward X-axis, a starboard Y-axis, and an upward Z-axis centrally aligned with the ship body axis). $\boldsymbol{R}$ represents the rotation matrix from the ship fixed frame to the geodetic coordinate system:

$$\boldsymbol{R} = \boldsymbol{R}_{\text{heading}} \cdot \boldsymbol{R}_{\text{pitch}} \cdot \boldsymbol{R}_{\text{roll}} = \begin{bmatrix} r_{11} & r_{12} & r_{13} \\ r_{21} & r_{22} & r_{23} \\ r_{31} & r_{32} & r_{33} \end{bmatrix}, \tag{3}$$

If the lever arms between the shipborne GNSS and the transceiver are known, Equation (2) can be substituted into (1) directly, and after linearising, the basic function model of GNSS-A positioning is obtained as follow:

$$\begin{array}{l} v = \left.\frac{\partial \rho}{\partial x_{\text{floor}}}\right|_{X_{\text{floor\_0}}} \cdot \mathrm{d}x_{\text{floor}} + \left.\frac{\partial \rho}{\partial y_{\text{floor}}}\right|_{X_{\text{floor\_0}}} \cdot \mathrm{d}y_{\text{floor}} + \left.\frac{\partial \rho}{\partial z_{\text{floor}}}\right|_{X_{\text{floor\_0}}} \cdot \mathrm{d}z_{\text{floor}} + \left(\rho_0 - \text{vos} \cdot \frac{\text{t}}{2}\right), \\ = \mathrm{a}_1 \cdot \mathrm{d}x_{\text{floor}} + \mathrm{a}_1 \cdot \mathrm{d}y_{\text{floor}} + \mathrm{a}_1 \cdot \mathrm{d}z_{\text{floor}} + \mathrm{l} \end{array} \tag{4}$$

where $\boldsymbol{X}_{\text{floor\_0}}$ represents the initial values of unknown parameters (such as $x_{floor}$, $y_{floor}$, and $z_{floor}$), $\rho_0$ means the geometrical distance calculated by $\boldsymbol{X}_{\text{floor\_0}}$. $a_1$, $a_2$, and $a_3$ represent $\left.\frac{\partial \rho}{\partial x_{\text{floor}}}\right|_{X_{\text{floor\_0}}}$, $\left.\frac{\partial \rho}{\partial y_{\text{floor}}}\right|_{X_{\text{floor\_0}}}$ and $\left.\frac{\partial \rho}{\partial z_{\text{floor}}}\right|_{X_{\text{floor\_0}}}$ respectively, which are the partial derivatives of the observation to each unknown parameter at $\boldsymbol{X}_{\text{floor\_0}}$. $l$ represents the constant term in the function model. $v$ denotes the residual error of each observation.

The velocity of sound in seawater is about 1500 m/s and varies in space and time. This characteristic affects the distance inversion between the acoustic transceiver and transponder, and then the sound velocity bias becomes one of the leading systematic errors for underwater acoustic positioning. Generally, both the shipborne acoustic transceiver and GNSS equipment are installed on site. Thus, the transceiver lever arms are obtained by accumulating measurements in the different directions of the ship fixed frame. Owing to the offset error caused by installation, the lever arms measured are inaccurate, which is another main systematic error. With redundant observation information, the lever arm offset can be set as parameters with sound velocity correction and transponder position. Thus, the observation equation can be expressed as follows:

$$\begin{array}{c} v + (\text{vos}_0 + dvos) \cdot \frac{t}{2} = \\ \sqrt{(x_{\text{floor}} - x_{\text{surface}})^2 + (y_{\text{floor}} - y_{\text{surface}})^2 + (z_{\text{floor}} - z_{\text{surface}})^2}, \end{array} \tag{5}$$

where the 3-D coordinate of the transceiver contains unknown parameters to be solved, $\Delta x$, $\Delta y$ and $\Delta z$:

$$\begin{cases} x_{\text{surface}} = x_{\text{GNSS}} + r_{11} \cdot \Delta x + r_{12} \cdot \Delta y + r_{13} \cdot \Delta z \\ y_{\text{surface}} = y_{\text{GNSS}} + r_{21} \cdot \Delta x + r_{22} \cdot \Delta y + r_{23} \cdot \Delta z \\ z_{\text{surface}} = z_{\text{GNSS}} + r_{31} \cdot \Delta x + r_{32} \cdot \Delta y + r_{33} \cdot \Delta z \end{cases}, \tag{6}$$

By linearizing the observation equations, Equation (7) can be derived, and then the improved function model of GNSS-A positioning can be expressed with (9). Based on the least square principle, the parameters can be determined with (10):

$$\begin{array}{c} v = a_1 \cdot dx_{\text{floor}} + a_2 \cdot dy_{\text{floor}} + a_3 \cdot dz_{\text{floor}} + b_1 \cdot d\Delta x + b_2 \cdot d\Delta y + b_3 \cdot d\Delta z \\ -\frac{t}{2} dvos + \left(\rho_0 - \text{vos}_0 \cdot \frac{t}{2}\right) \end{array} \tag{7}$$

$$\begin{cases} \mathrm{b}_1 = a_1 \cdot (r_{11} + r_{21} + r_{31}) \\ \mathrm{b}_2 = a_2 \cdot (r_{12} + r_{22} + r_{32}) \\ \mathrm{b}_3 = a_3 \cdot (r_{13} + r_{23} + r_{33}) \end{cases} \tag{8}$$

$$\begin{bmatrix} v_1 \\ v_2 \\ \vdots \\ v_n \end{bmatrix} = \begin{bmatrix} a_{11} & a_{12} & a_{13} & b_{11} & b_{12} & b_{13} & -\frac{t_1}{2} \\ a_{21} & a_{22} & a_{23} & b_{21} & b_{22} & b_{23} & -\frac{t_2}{2} \\ \vdots & \vdots & \vdots & \vdots & \vdots & \vdots & \vdots \\ a_{\text{n1}} & a_{\text{n2}} & a_{\text{n3}} & b_{\text{n1}} & b_{\text{n2}} & b_{\text{n3}} & -\frac{t_n}{2} \end{bmatrix} \cdot \begin{bmatrix} dx \\ dy \\ dz \\ d\Delta x \\ d\Delta y \\ d\Delta z \\ dvos \end{bmatrix} + \begin{bmatrix} \mathrm{l'}_1 \\ \mathrm{l'}_2 \\ \vdots \\ \mathrm{l'}_n \end{bmatrix} = \boldsymbol{A} \cdot d\boldsymbol{X} + \boldsymbol{L} \tag{9}$$

$$\hat{\boldsymbol{X}} = \boldsymbol{X}_0 + d\boldsymbol{X} = \boldsymbol{X}_0 + \left(\boldsymbol{A}^T \boldsymbol{P} \boldsymbol{A}\right)^{-1} \left(\boldsymbol{A}^T \boldsymbol{P} \boldsymbol{L}\right). \tag{10}$$

## 3. Experimental Data

For verifying the GNSS-A positioning method, this paper utilised data from a sea trial carried out near Lingshan Island, Qingdao, China, on December 1, 2017. The data mainly included the GNSS dynamic positioning results, ship attitude, travel times of acoustic signals, measured lever arm from the GNSS reference point to the transceiver, and sound velocity profiles. Position and attitude information of the survey ship was obtained using the POS MV 320 system from the Applanix Company. Based on post-processed kinematic technology, the position of the system reference point can be acquired, and the results of ship attitude can be obtained from the inertial navigation system and GNSS of the POS MV. The positioning results illustrate that the mean Standard Deviation (STD) of each epoch in the northing, easting, and height directions were 1.1, 1.0, and 2.8 cm, respectively. For the hull attitude results, the mean STD were 0.02°, 0.01°, and 0.01° for heading, pitch, and roll, respectively. According to the predetermined ship sailing track (a circle with cross shown in Figure 2), the measurements were collected for the following model discussion. The period of the selected data was about 77 min, during which the sound velocity in seawater was measured by SV PlusV2 sound velocity profiler of the AML Oceanographic Company. Figure 3 shows the sound velocity profiles, where the blue points represent the original sound velocity observed during the trial period, and the red dotted line represents the weighted mean sound velocity (1454.067 m/s), which was calculated from the original observations. Considering our trial was carried out in the shallow sea (about 25 m), it is safe to fix the weighted mean sound velocity as the prior value in subsequent calculations. The sea state on the trial day was fine, from Calm to Smooth, but there was a sound velocity spring layer (about 2.5 m/s) at the depth 5–10 m from the sea surface, and the sound velocity increased rapidly from 1447 m/s to 1455 m/s, which may be caused by the large sea current in the trial area.

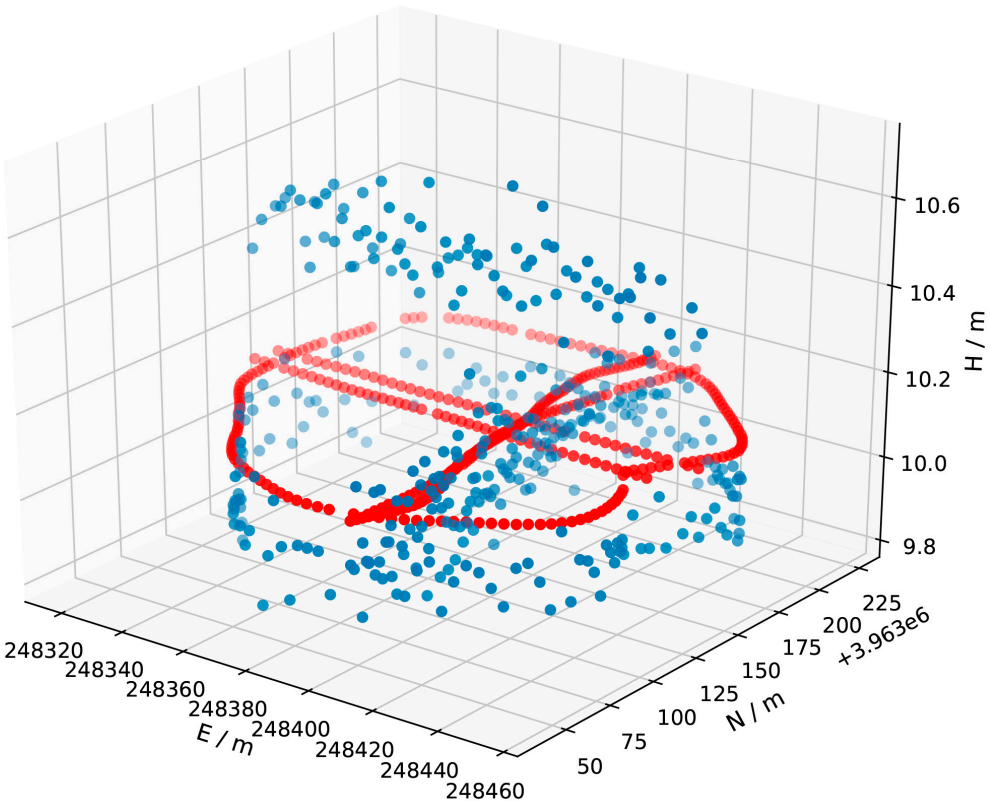


**Figure 2.** The section of the ship's 3-D sailing track diagram (the blue points, which are scattered and do not display the regular geometry, denote the 3-D track position of the ship; the red points, which present clearly circle and cross tracks, are the projections of blue points to the average height plane; the depth of the dot colour represents the distance from the perspective).

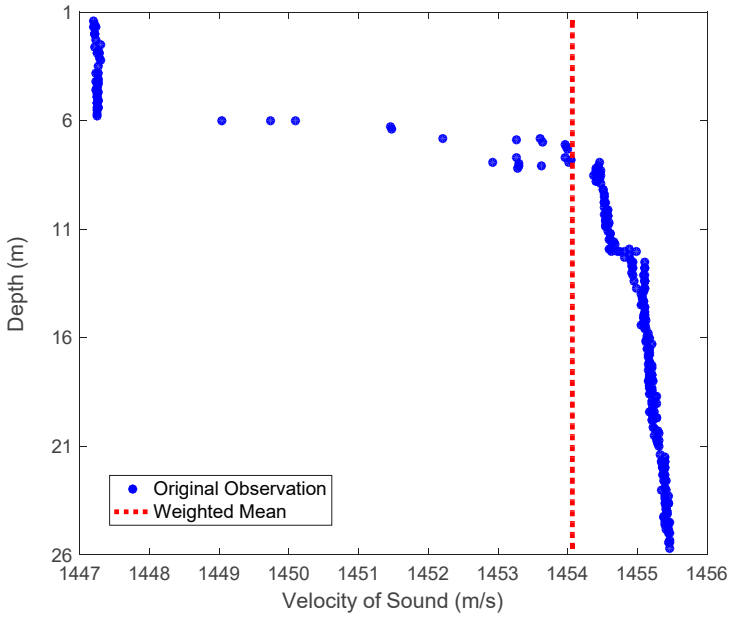


**Figure 3.** The sound velocity profiles.

## 4. Questions Raised

The two main errors, i.e., the offset errors of the shipborne equipment and sound velocity bias, exist in the measurements, whereas the ranges of such errors are unclear. To discuss the influences of these errors on the position results of the seafloor transponder, they were estimated as unknown parameters with the seafloor station's 3-D position. Assuming the lever arms and velocity of sound have no error, then the parameters that need to be estimated are just 3-D coordinates of the seafloor transponder. In this case, the error equation is (4), and this solution model is called the NEH model, where N, E, and H represent the coordinate components of the transponder position in the northing, easting, and height directions, corresponding to $X_{\text{floor}}$, $Y_{\text{floor}}$, and $Z_{\text{floor}}$, respectively. If errors exist in the transceiver lever arms, but no error exists in the sound velocity, the three offset components of the lever arms can be solved together with the 3-D position of the seafloor station. In this case, the error equation is (7) without the *dvos* parameter, and this solution model is called the NEH+dxyz model, where dxyz means including three transceiver lever arms in the model and x, y, and z correspond to $\Delta x$, $\Delta y$, and $\Delta z$, respectively. When an error exists in the sound velocity, but no error in the lever arms, the sound velocity correction parameter and the 3-D coordinates of seafloor transponder should be solved together. Then, the error equation can be written as (7) without the lever arm parameters, and this solution model is called the NEH+dv model, where dv indicates including the parameter of the velocity of sound in the model, corresponding to *dvos*. It should be noted that for those variables not estimated in certain models, they are fixed in the observation equation as initial values (measured during the trial).

The observation data were processed by the NEH, NEH+dxyz, and NEH+dv models, and their results are summarised in Table 1. According to the table, significant differences in the three model's results were observed, especially in the vertical direction. The NEH model's results feature a higher STD (about 0.12 m in horizontal and 0.24 m in vertical). Adding the lever arm parameter can reduce the STD, but the results of the vertical parameter (vertical components of transceiver lever arms and seafloor transponder) in the NEH+dxyz model appear to be abnormal, which may be due to the high correlation of vertical parameters. The results of the NEH+dv model demonstrated a considerable acoustic velocity correction parameter, suggesting a problem with the acoustic velocity value, which may be caused by the un-calibration of the acoustic velocity profiler. As the experiment was carried out in a shallow water area, where the ship track covered a small area and lasted a short period, the

acoustic velocity was deemed to exhibit a relatively small variation in both time and space. As the ship sails along the predetermined symmetrical tracks, the effects of sound velocity errors in the horizontal direction can be mostly eliminated in adjustment, and residual influences can be considered as fixed values in the vertical direction.

**Table 1.** Results of Three Estimation Model (Unit: m. NEH represent the coordinate components of the transponder position in the northing, easting, and height directions, including N, E, and H; dxyz means three components of transceiver lever arms in the ship-fixed coordinate system, including deltaX, deltaY, and deltaZ; dv indicates the velocity of sound, dvos; STD means the standard deviation of the estimate.).

| Parameter Name | NEH Model | | NEH+dxyz Model | | NEH+dv Model | |
|---|---|---|---|---|---|---|
| | Estimate | STD | Estimate | STD | Estimate | STD |
| N | 3963161.343 | 0.112 | 3963161.328 | 0.072 | 3963162.401 | 0.063 |
| E | 248380.512 | 0.136 | 248380.397 | 0.089 | 248380.164 | 0.068 |
| H | −14.902 | 0.242 | −20.961 | 4.453 | −17.868 | 0.134 |
| deltaX | - | - | 4.197 | 0.256 | - | - |
| deltaY | - | - | 3.179 | 0.259 | - | - |
| deltaZ | - | - | −13.504 | 4.436 | - | - |
| dvos | - | - | - | - | 43.014 | 1.245 |

## 5. Error Correction Method

### *5.1. Transceiver Lever Arms Correction*

The transceiver lever arm is a 3-D vector in the ship fixed frame. Because the observation data were collected according to the predetermined sailing track, the heading information varied regularly, and the influences of the transceiver lever arm offset on the positioning manifested as a periodic variation in the horizontal direction. Owing to the dynamic environment of the sea surface, the roll and pitch angles of the ship varied randomly with time. Thus, the influences of the transceiver lever arm offset showed stochastic properties. Given the existence of lever arm offsets, evaluating the performance of the estimation model is difficult, and the estimation of the sound velocity correction parameter is also affected. As the influence of sound velocity error is mainly fixed in the vertical direction, the estimation of the transducer lever arm was analysed first.

In the NEH+dxyz model, the vertical direction parameters, including the height of seafloor transponder and vertical lever arm parameter, are abnormal. To explore the reasons for the anomalous transponder height and transceiver lever arm in the vertical direction, the correlation of the parameters in the NEH+dxyz model was shown in Figure 4. High correlations existed between the three lever arm parameters and the seafloor station height (larger than 0.90), and the seafloor station height was completely correlated with the vertical lever arm. In the NEH+dxyz model, only the vertical parameter results were abnormal. Thus, the high correlation between the two parameters in the vertical direction produced an abnormal solution.

The vertical lever arm is strongly correlated with the seafloor station's height. As the magnitude of lever arm errors cannot be measured precisely, its correction parameter cannot be constrained effectively, thereby increasing uncertainty in the estimation. Considering the lever arm results of the NEH+dxyz model, we proposed a sample search method. Firstly, a search space, centred on the measurement, is established for the vertical lever arm parameter. Then, values in the search space are successively extracted out as the test object, with a fixed interval, and fixed in the observation equation to complete the estimation process. Considering that the mean square error of unit weight, an index of the residual error of observations, can be used to represent the size of unmodeled errors in the observations, we select the vertical lever arm parameter that minimises the mean square error of unit weight as the search result and set it as the fixed prior value for subsequent calculations. As almost every coefficient in the error equation is affected by the vertical lever arm, the mathematical expression

of the relation between the vertical lever arm and the mean square error of the unit weight cannot be derived. Therefore, the aim of decoupling the vertical component cannot be reached algebraically, while our sample search method offers a good solution numerically. In this experiment, the search space was set within 2 m around –8.118 m, and the sample search was performed at an interval of 0.001 m. Figure 5 shows the relationship between the vertical lever arm parameter and the mean square error of the unit weight. The optimal value of −7.772 m for the vertical lever arm was obtained. However, the values of the mean square error of unit weight are very high (larger than 0.94 m), which means that there are still unmodeled errors in the observations, and they are independent of the vertical lever arm.

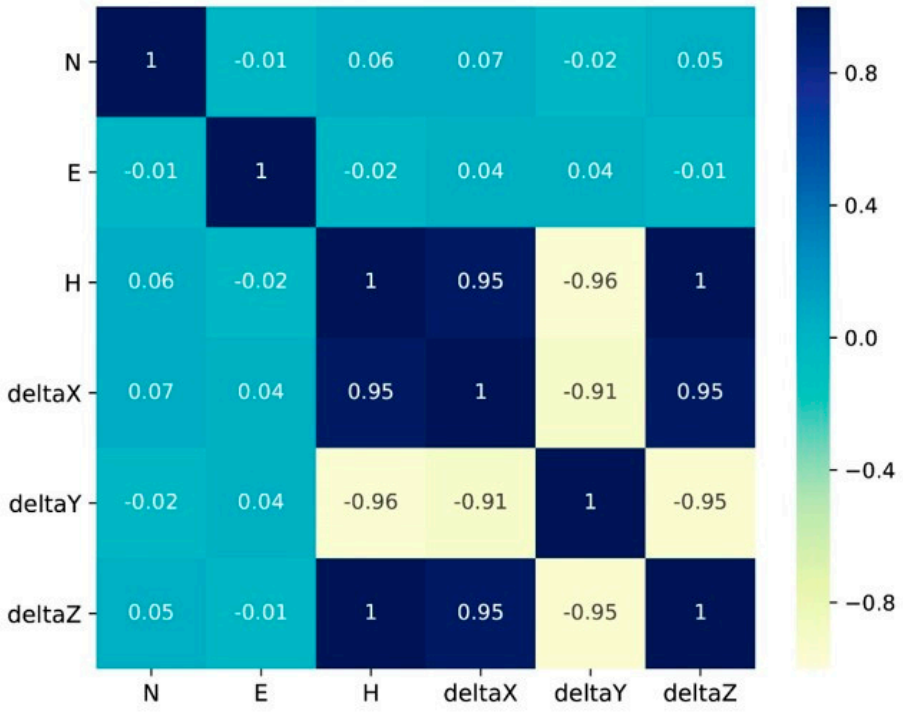


**Figure 4.** The correlation coefficient of the parameters.

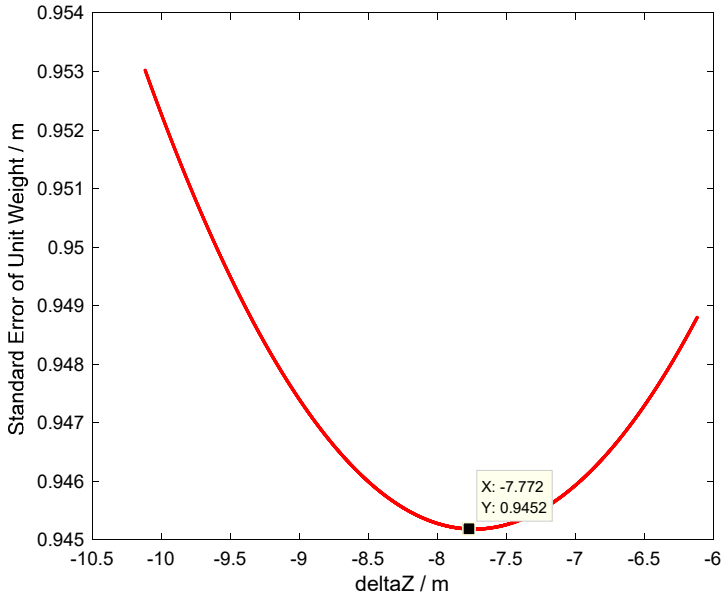


**Figure 5.** The relation between the vertical lever arm and the mean square error of unit weight.

The vertical lever arm parameter searched was used as a fixed value to carry out the NEH estimation model and the NEH+dxy model, in which the NEH+dxyz model becomes the NEH+dxy model after removing the vertical lever arm parameter. It should be noted that the NEH+dxyz model was abandoned in the following study because of its abnormal estimate in the vertical orientation. Table 2 shows the statistical results, where the above two methods were normal. The STD of the N and E parameters reduced from 11 to 13 cm in the NEH model to 7 to 8 cm in the NEH+dxy model, and that of the H parameter improved from 24 cm to 15 cm. The residual errors of the two methods are summarised in Table 3, which shows that adding horizontal transceiver lever arm offset parameters could significantly reduce the mean and STD of the residual error to around 0.27 m and 0.90 m, respectively. However, the two indicators were still relatively large, just like the mean square error of the unit weight shown in Figure 5, indicating that significant systematic errors still existed.

**Table 2.** Results of Two Estimation Model (Unit: m).

| Parameter Name | Initial Value | NEH Model | | NEH+dxy Model | |
|---|---|---|---|---|---|
| | | Estimate | STD | Estimate | STD |
| N | 3963134.860 | 3963161.344 | 0.111 | 3963161.333 | 0.072 |
| E | 248394.141 | 248380.510 | 0.135 | 248380.397 | 0.089 |
| H | −19.246 | −14.430 | 0.238 | −15.212 | 0.159 |
| deltaX | 5.820 | - | - | 4.513 | 0.077 |
| deltaY | 1.706 | - | - | 2.860 | 0.077 |

**Table 3.** Residual Error of Two Estimation Model (Unit: m).

| Parameter Name | NEH Model | NEH+dxy Model |
|---|---|---|
| Average | 0.488 | 0.267 |
| STD | 1.373 | 0.902 |

### *5.2. Sound Velocity Correction and its Combination with Lever Arms Correction*

Based on the geometric distances inverted from the sound travel time, the GNSS-A positioning technique determines the unknown parameters. The estimated parameters will absorb unmodeled errors when the model is inaccurate. Although the NEH+dxy model significantly improves the precision, the statistical indicators of its residual errors still suggest the existence of a systematic unmodeled bias in the observation equations. The results of the NEH+dv model revealed a significant deviation to the sound velocity measurement, which is assumed to be caused by the improper calibration of the sound velocity profiler. Compared with the NEH model, the average residual error of the NEH+dv model was much smaller and close to zero, indicating that the sound velocity correction parameter absorbs system biases, and the STD of residual errors also showed a significant decrease from 1.373 m to 0.713 m, suggesting that the model was improved. The sound velocity correction parameter directly corrects errors in the signal propagation path, not only reflecting systematic errors in the sound velocity but also absorbing other unmodeled systematic deviations, such as hardware delay errors.

As the NEH+dv model omits the transceiver lever arm parameter, the sound velocity correction parameter is affected by the ship attitude variation. Therefore, sound velocity correction was added to the measurement equations and estimated together with the three position parameters and two horizontal lever arm parameters, forming the NEH+dv+dxy model. The vertical lever arm value from the sample search was set as fixed. The results of the NEH+dv and the NEH+dv+dxy models are shown in Table 4. The STD of the NEH+dv model in Table 4 (6–7 cm in the horizontal orientation, around 13 cm in the vertical orientation) is much better than that of the NEH model in Table 1. The NEH+dv model shows a similar positioning level with that of the NEH+dxy model, which means that the NEH+dv model makes a similar degree of improvement for estimation with the NEH+dxy model. The sound velocity correction was 40.761 m/s. Adding the sound velocity correction can improve the

parameter estimation precision to the millimetre level in the horizontal direction and about 1 cm in the vertical direction. Figure 6 shows the time series of the residual errors for the NEH+dv, NEH+dxy, and NEH+dv+dxy models. As the figure is displayed when only the transceiver lever arm offsets or the sound velocity biases were considered with the transponder 3-D coordinates, the residual error was large and highly related to the ship's sailing track, which could be attributed to the remaining systematic errors in the observation. Meanwhile, the residual errors of the NEH+dv model and the NEH+dxy model are similar in size, which verifies the similar degree of estimation improvement. When these two errors were both taken into account, the residual errors fluctuated around the zero value and with a small fluctuation range (5.6 cm), indicating that the systematic errors had been mostly eliminated.

**Table 4.** Results of Two Estimation Models (Unit: m).

| Parameter Name | Initial Value | NEH+dv Model | | NEH+dxy+dv Model | |
|---|---|---|---|---|---|
| | | Estimate | STD | Estimate | STD |
| N | 3963134.860 | 3963162.390 | 0.062 | 3963162.240 | 0.005 |
| E | 248394.141 | 248380.165 | 0.067 | 248379.956 | 0.006 |
| H | −19.246 | −17.368 | 0.131 | −17.208 | 0.011 |
| deltaX | 5.820 | - | - | 4.688 | 0.005 |
| deltaY | 1.706 | - | - | 1.634 | 0.006 |
| dvos | 0.000 | 42.589 | 1.219 | 40.761 | 0.133 |

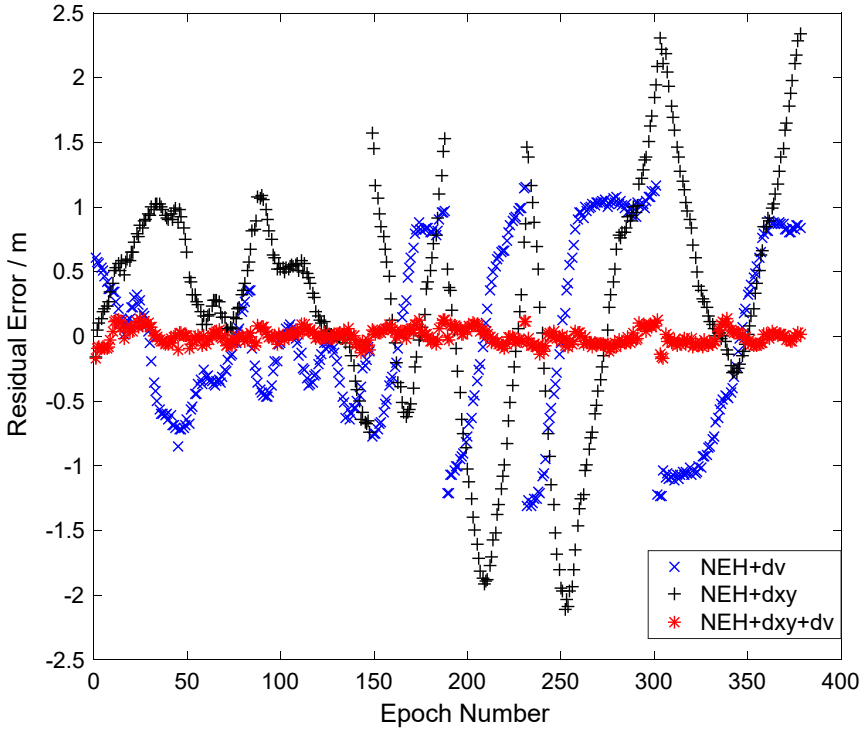


**Figure 6.** Time series of residual errors for the three models.

## 6. Conclusions

As the infrastructure of seafloor navigation and positioning, the seafloor geodetic station relies on the GNSS-A positioning technique to obtain its precise position. However, under a situation with a large offset of transceiver lever arms and a significant bias in sound velocity measurement, the positioning accuracy of the GNSS-A technique will be deteriorated by these two systematic errors. To cope with these problems, this paper analysed the function model of GNSS-A positioning for the seafloor station

and studied the processing methods of the offset error of transceiver lever arms and the bias of sound velocity. By adding the corresponding parameters to be solved, the high correlation between the vertical lever arm parameter and seafloor station height was revealed. Then, a sample search method was proposed for offset parameter determination in the vertical direction, which obtained significant estimation improvements. To correct the bias of the sound velocity profile and reduce the influence of the unmodeled error, the sound velocity correction parameter was added in the estimation, and the positioning precision was remarkably improved. Finally, by combining the sample search method and adding parameters for the horizontal lever arms and sound velocity correction, the accuracy of the seafloor position parameters was improved from 6 to 9 cm in the horizontal position and 13 to 16 cm in the vertical position to better than 1 cm, which verified the proposed data processing methods.

**Author Contributions:** Conceptualization, G.C., Y.L. (Yang Liu), and Y.X.L. (Yanxiong Liu); methodology, G.C., Y.X.L. and Y.L.; software, G.C.; validation, G.C., Y.L. and Y.X.L.; formal analysis, G.C.; investigation, G.C., Z.T. and M.L.; resources, G.C., Y.X.L., Z.T. and M.L.; data curation, G.C. and Y.L.; writing—original draft preparation, G.C.; writing—review and editing, Y.X.L. and Y.L.; supervision, Y.X.L. and Z.T.; project administration, Y.X.L. and Y.L.; funding acquisition, Y.X.L. and Y.L.

**Funding:** This research was funded by the National Key Research and Development Program of China (Grant No. 2016YFB0501703) and Basic Scientific Fund for National Public Research Institutes of China (Grant No. 2018Q04).

**Acknowledgments:** We thank Harbin Engineering University, National Deep Sea Centre of China and Shanghai Acoustic Laboratory of the Chinese Academy of Sciences for their help and participation in the sea trial. The authors gratefully acknowledge Associate Professor Cuie Zheng and Lecturer Ming Shi at Harbin Engineering University, and Senior Engineer Minyan Huang at Shanghai Acoustic Laboratory for their support in data processing and analysis.

**Conflicts of Interest:** The authors declare no conflict of interest.

## References

1. Yang, F.; Lu, X.; Li, J.; Han, L.; Zheng, Z. Precise positioning of underwater static objects without sound speed profile. *Mar. Geod.* **2011**, *34*, 138–151. [CrossRef]
2. Zhou, Y.; Wang, C.; Zhu, J.; Li, Q. Optimal sensor configuration for positioning seafloor geodetic node. *Ocean. Eng.* **2017**, *142*, 1–9. [CrossRef]
3. Torge, W.; Müller, J. Methods of measurement. In *Geodesy*, 4th ed.; Walter de Gruyter: Berlin, Germany, 2012; pp. 113–222.
4. Bürgmann, R.; Chadwell, D. Seafloor geodesy. *Annu. Rev. Earth Planet. Sci.* **2014**, *42*, 509–534. [CrossRef]
5. Leonard, J.J.; Bahr, A. Autonomous Underwater Vehicle Navigation. In *Springer Handbook of Ocean Engineering*, 1st ed.; Dhanak, M.R., Xiros, N.I., Eds.; Springer: New York, NY, USA, 2016; pp. 341–357.
6. Thomson, D.J.M.; Dosso, S.E.; Barclay, D.R. Modeling AUV localization error in a long baseline acoustic positioning system. *IEEE J. Ocean. Eng.* **2018**, *43*, 955–968. [CrossRef]
7. Tan, H.; Diamant, R.; Seah, W.K.G.; Waldmeyer, M. A survey of techniques and challenges in underwater localization. *Ocean. Eng.* **2011**, *38*, 14–15. [CrossRef]
8. Han, Y.; Li, Z.; Zheng, C.; Shun, D. A precision evaluation method of USBL positioning systems based on LBL triangulation. *Acta Phys. Sin.* **2015**, *64*, 094301.
9. Xu, P.; Ando, M.; Tadokoro, K. Precise, three-dimensional seafloor geodetic deformation measurements using difference techniques. *Earth Planets Space* **2005**, *57*, 795–808. [CrossRef]
10. Wu, Y. Study on Theory and Method of Precise LBL Positioning Software System. Ph.D. Thesis, Wuhan University, Wuhan, China, 2013.
11. Yamada, T.; Ando, M.; Tadokoro, K.; Sato, K.; Okuda, T.; Oike, K. Error evaluation in acoustic positioning of a single transponder for seafloor crustal deformation measurements. *Earth Planets Space* **2002**, *54*, 871–881. [CrossRef]
12. Chadwell, C.D. Shipboard towers for Global Positioning System antennas. *Ocean. Eng.* **2003**, *30*, 1467–1487. [CrossRef]
13. Kussat, N.H.; Chadwell, C.D.; Zimmerman, R. Absolute positioning of an autonomous underwater vehicle using GPS and acoustic measurements. *IEEE J. Ocean. Eng.* **2005**, *30*, 153–164. [CrossRef]

14. Liu, Y.; Peng, L.; Wu, Y.; Zhou, X. Calibration of transducer and transponder positions. *Geomat. Inf. Sci. Wuhan Univ.* **2006**, *31*, 610–612.
15. Zhang, K.; Li, Y.; Zhao, J.; Rizos, C. Underwater Navigation Based on Real-time Simultaneous Sound Speed Profile Correction. *Mar. Geod.* **2016**, *39*, 98–111. [CrossRef]
16. Urick, R.J. *Principles of Underwater Sound*, 3rd ed.; McGraw-Hill: New York, NY, USA, 1983.
17. Sun, W.; Yin, X.; Bao, J.; Zeng, A. Semi-parametric adjustment model methods for positioning of seafloor control point. *Acta Geod. Cartogr. Sin.* **2019**, *48*, 117–123.
18. Wang, X.; Khazaie, S.; Komatitsch, D.; Sagaut, P. Sound-source localization in range-dependent shallow-water environments using a four-layer model. *IEEE J. Ocean. Eng.* **2019**, *44*, 220–228. [CrossRef]
19. Diamant, R.; Lampe, L. Underwater Localization with Time-Synchronization and Propagation Speed Uncertainties. *IEEE Trans. Mob. Comput.* **2013**, *12*, 1257–1269. [CrossRef]
20. Chadwell, C.D.; Spiess, F.N. Plate motion at the ridge-transform boundary of the south cleft segment of the Juan de Fuca Ridge from GPS-acoustic data. *J. Geophys. Res. Solid Earth* **2008**, *113*, B04415. [CrossRef]
21. Fujita, M.; Ishikawa, T.; Mochizuki, M.; Sato, M.; Toyama, S.; Katayama, M.; Kawai, K.; Matsumoto, Y.; Yabuki, T.; Asada, A.; et al. GPS/Acoustic seafloor geodetic observation: Method of data analysis and its application. *Earth Planets Space* **2006**, *58*, 265–275. [CrossRef]
22. Yokota, Y.; Ishikawa, T.; Sato, M.; Watanabe, S.; Saito, H.; Ujihara, N.; Matsumoto, Y.; Toyama, S.; Fujita, M.; Yabuki, T.; et al. Heterogeneous interplate coupling along the Nankai Trough, Japan, detected by GPS-acoustic seafloor geodetic observation. *Prog. Earth Planet. Sci.* **2015**, *2*, 10. [CrossRef]
23. Zheng, C.; Shun, D.; Zhang, D.; Li, X. Research the calibration technology of the installation error in ultra-short baseline acoustic positioning system. *Comput. Eng. Appl.* **2007**, *43*, 171–173.
24. Chen, H.; Wang, C. Optimal localization of a seafloor transponder in shallow water using acoustic ranging and GPS observations. *Ocean. Eng.* **2007**, *34*, 2385–2399. [CrossRef]
25. Zhang, J.; Han, Y.; Zheng, C.; Sun, D. Underwater target localization using long baseline positioning system. *Appl. Acoust.* **2016**, *111*, 129–134. [CrossRef]
26. Gagnon, K.; Chadwell, C.D.; Norabuena, E. Measuring the onset of locking in the Peru–Chile Trench with GPS and acoustic measurements. *Nature* **2005**, *434*, 205–208. [CrossRef] [PubMed]
27. Yokota, Y.; Ishikawa, T.; Watanabe, S.; Tashiro, T.; Asada, A. Seafloor geodetic constraints on interplate coupling of the Nankai Trough megathrust zone. *Nature* **2016**, *534*, 374–377. [CrossRef] [PubMed]
28. Zhao, J.; Zhou, Y.; Zhang, H.; Wu, Y.; Fang, S. A new method for absolute datum transfer in seafloor control network measurement. *J. Mar. Sci. Technol.* **2016**, *21*, 216–226. [CrossRef]
29. Zhao, S.; Wang, Z.; He, K.; Ding, N. Investigation on underwater positioning stochastic model based on acoustic ray incidence angle. *Appl. Ocean. Res.* **2018**, *77*, 69–77. [CrossRef]
30. Han, Y.; Zheng, C.; Shun, D. A high precision calibration method for long baseline acoustic positioning systems. *Chin. J. Acoust.* **2017**, *36*, 489–500.